Comparison of Si Doping Effect on GaN Nanowires and Films Synthesized by Metal-Organic Chemical Vapor Deposition

Jongsun Maeng, Min-Ki Kwon, Soon-Shin Kwon, Gunho Jo, Sunghoon Song,
Tae-Wook Kim, Byung Sang Choi, Seong-Ju Park, and Takhee Lee*

*Department of Materials Science and Engineering, Gwangju Institute of Science and Technology,
Gwangju 500-712, Korea*

We investigated Si doping effect on GaN nanowires and GaN films grown by metal-organic chemical vapor deposition (MOCVD). Si as *n*-type dopant is incorporated to GaN nanowires and GaN films controlled by SiH_4 flow rate (0, 1, 5, 8, and 10 sccm). The charge concentration and mobility of GaN films increased and decreased, respectively, as increasing the SiH_4 flow rate, whereas those for GaN nanowires were not influenced by the SiH_4 flow rate. Significant vacancies and impurities resulted in the intense yellow band in GaN nanowires as compared with GaN films, which leads to the large device-to-device variation and negligible dependence of Si doping and the SiH_4 flux rate on the electrical properties of GaN nanowires.

Keywords: GaN, Nanowire, MOCVD.

1. INTRODUCTION

Recently, one dimensional nanomaterials have attracted much attentions due to the potential applications in nanoscale optoelectronic devices.[1,2] Integration of several semiconductor nanowires devices with Si-based electronic devices will be potential for on-chip integration of various functional nanomaterial devices.[3] Among these materials, the GaN nanostructures, having a direct wide band gap ∼3.4 eV and good thermal stability is very suitable for the areas of high temperature devices, light emitting diodes, and lasers.[4] Various approaches for formation of GaN nanowires have been employed, which include catalytic reaction of Ga metal and ammonia, molecular beam epitaxy, metal-organic chemical vapor deposition (MOCVD), hydride vapor epitaxy, and laser ablation.[5–9] Typically, metal-assisted catalytic reaction is used to initiate nanowire growth based on a vapor-liquid-solid (VLS) or vapor-solid-solid (VSS) mechanism.[9,10] The size of catalytic nanoparticles of Au, Ni, or Fe can control diameter of nanowires.[9] Typically, the electrical characteristics of as-grown GaN nanowires by hot-wall chemical vapor deposition (CVD) are unintentionally *n*-type with large carrier concentrations of 10^{18}–10^{19} cm^{-3}.[5] On the contrary, the MOCVD technique in III-nitride film technology can

offer a radial heterostructure growth and doping control using precursor delivery for GaN nanowires growth.[4,11]

In this work, we report the synthesis of GaN nanowires with $[11\bar{2}0]$ growth orientation on oxidized Si substrate by MOCVD method. We compare the Si doping effect on the electrical and optical properties in GaN films and GaN nanowires by control of the SiH_4 flow rate (0, 1, 5, 8, and 10 sccm). Scanning electron microscopy (SEM), transmission electron microscopy (TEM), and selected area electron diffraction (SAED) were used to investigate structural properties, such as morphology, crystallinity, growth direction, and defect information. We extracted the electrical properties of GaN film and GaN nanowires by Hall measurements and by characterizing nanowire field effect transistors, respectively. Photoluminescence (PL) on GaN films and micro-photoluminescence (μ-PL) on individual GaN nanowires were employed to characterize their optical properties.

2. EXPERIMENTAL DETAILS

2.1. Synthesis of GaN Nanowires

GaN nanowires were synthesized by VLS growth mechanism using MOCVD in a rotating-disc cold-wall reactor. Ni nanoparticles as catalysts were created by depositing a thin Ni film (∼2 nm thick) on thermally grown

---

*Author to whom correspondence should be addressed.

oxidized silicon wafer using an e-beam evaporator. After catalyst deposition, the wafer was loaded into the reactor for nanowire growth. GaN nanowires were grown at the temperature of 750 °C in hydrogen ambient. The flow rate of trimethylgallium (TMG) and ammonia (NH_3) was 116 μmol/min and 7600 sccm, respectively. The pressure was held constant at 200 Torr and the growth time was 30–40 min. Si doping was performed by controlling the flow rate of SiH_4 gas source (0, 1, 5, 8, and 10 sccm). GaN films were also grown at optimized epitaxial growth conditions.

The synthesized GaN nanowires were characterized using SEM (Hitachi S-4700), TEM (Philips CM 20T/STEM high-resolution TEM at 200 kV), and SAED to obtain structural information. SEM images of GaN nanowires were taken directly from the nanowire growth substrate. Nanowires were mechanically detached from the growth substrate by sonication in isopropyl alcohol and then were transferred on a holy carbon grid for TEM measurements. Similarly, individual nanowires were transferred from grown substrate onto a 600 nm-thick oxidized silicon substrate for μ-PL measurements. This substrate was selected because it does not show significant PL signal in spectral ranges of GaN. μ-PL spectroscopy was carried out using a Jobin Yvon LabRamHR system with 325 nm He-Cd laser as excitation source. The spatial resolution of the μ-PL spectroscopy was about a few μm using 40× objective lens.

2.2. Fabrication of GaN Nanowire Field Effect Transistors

GaN nanowires were fabricated as field effect transistors (FETs) in order to study their electrical properties, such as the carrier concentration and the carrier mobility. First, individual GaN nanowires suspended by sonicating the growth substrate for 30–60 s in isopropyl alcohol were dropped onto a 100 nm-thick thermally-grown oxide on silicon. The silicon substrate was a degenerate *p*-type substrate (resistivity ∼0.005 Ω-cm) that can serve as a common back gate electrode. Metal electrodes consisting of Ti (30 nm)/Au (70 nm) to produce ohmic contacts to GaN nanowires were then deposited by an e-beam evaporator, and defined as the source and drain electrodes by optical lithography and a lift-off process. The source and drain electrodes were patterned as an interdigitated electrode array, which have 32 interdigitated electrodes with spacing of 3 μm (Fig. 2). After forming electrodes, a rapid annealing was performed at 500 °C for 1 min in N_2 ambient to ensure the ohmic contact of the source and drain electrodes on GaN nanowires. Transistor properties such as source-drain current versus voltage characteristics as a function of gate voltage were measured using a semiconductor parameter analyser (Agilent B1500).

2.3. Preparation and Characterization of GaN Films

GaN films were grown on a (0001) sapphire substrate by low pressure MOCVD with a rotating-disk reactor (Emcore D125™). Detail description on growing GaN films has been discribed elsewhere.[12] The PL measurements were performed at room temperature with the 325 nm line of a focused continuous wave He-Cd laser as an excitation source. The luminescence was collected from the excited face and dispersed by a double monochromater and detected by a water-cooled photomultiplier tube followed by a gated photon counter. The electrical characteristics such as carrier concentration and mobility were obtained with Hall measurement system by the van der Pauw method.

3. RESULTS AND DISCUSSION

Typical GaN nanowires grown in our study are shown in Figure 1. The GaN nanowires grown by MOCVD have a tapered shape with smaller diameter at the Ni catalyst tip than at base (top left inset of Fig. 1(a)). Ni element was detected in energy dispersive spectroscope (EDS) spectrum
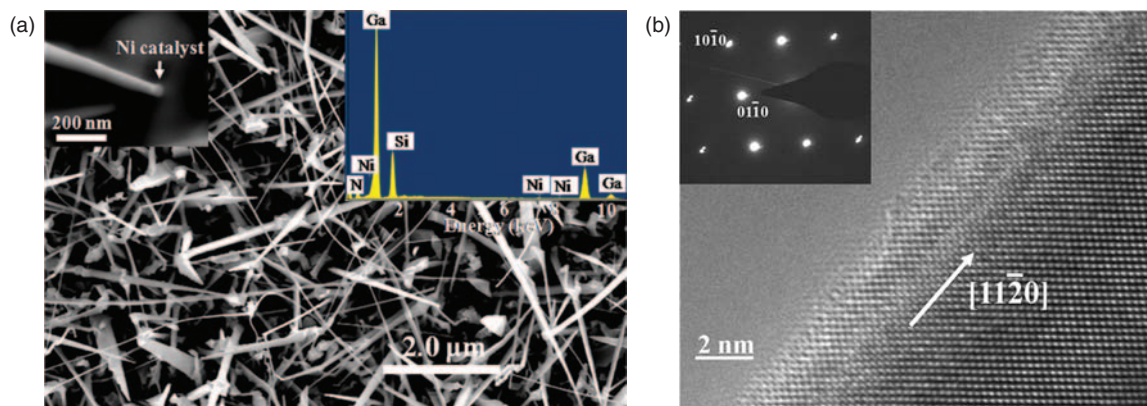
Fig. 1. (a) FE-SEM images of GaN nanowires grown by MOCVD, with a nanowire in tapered shape (right inset) and EDS spectrum at Ni catalyst tip (left inset). (b) High resolution TEM images and SAED pattern (inset) taken along [0001] the zone axis of a GaN nanowire.
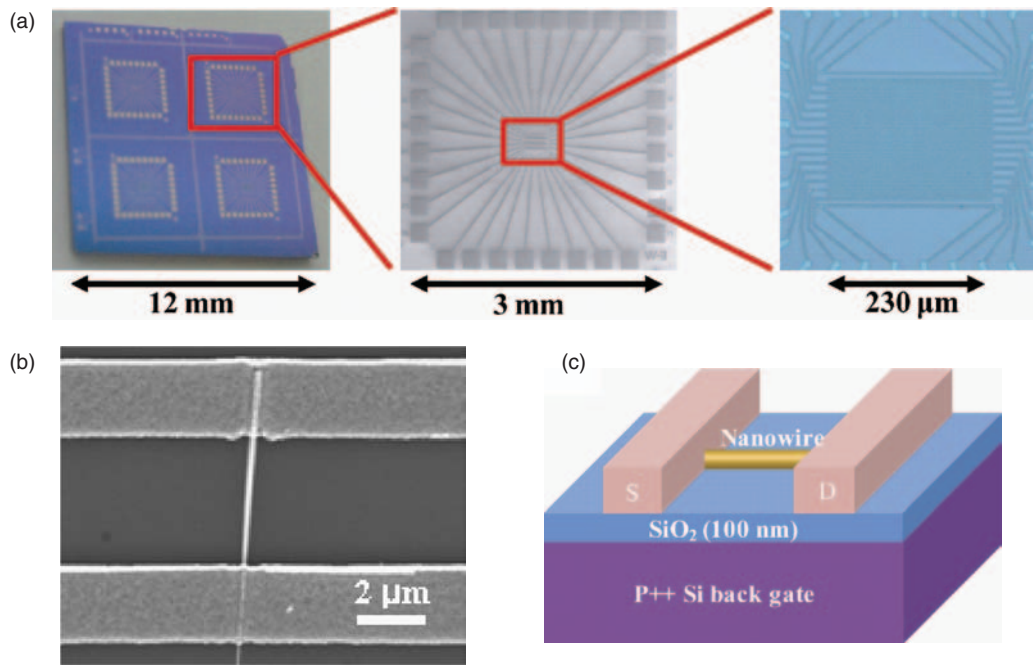
Fig. 2. (a) Optical and SEM images of GaN nanowire FET device. (b) SEM image of GaN nanowire channel of 3 μm in length. (c) Schematic diagram of a nanowire FET.

at the nanoparticle on a nanowire tip (right inset of Fig. 1(a)). Other elements such as Ga, N, and Si can be attributed to GaN nanowires and Si substrate. The catalytic nanoparticle on the nanowire tip (top left inset of Fig. 1(a)) is Ni, indicating a vapor-liquid-solid growth mechanism. The GaN nanowires have triangular cross-sections, smooth surfaces, and straight shape with size (diameter) ranging from 20–60 nm at the tips and 100–300 nm at the bases. The length of most nanowires is around 5–20 μm. To ensure the structural characteristics of the grown GaN nanowires, a high resolution transmission electron microscopy (HRTEM) images and SAED pattern of GaN nanowires were obtained, as shown in Figure 1(b). Clear lattice fringes indicate GaN nanowires are single crystalline. The nanowire growth direction was found to be [11$\bar{2}$0] from indexing the SAED patterns (inset of Fig. 1(b)). The lattice spacing was found to be ~0.32 nm between adjacent lattice planes, which corresponds to the distance between two (11$\bar{2}$0) crystal planes.

In order to investigate electrical properties of GaN nanowires such as carrier density and carrier mobility by Si doping effect, samples were prepared as nanowire FETs with back gate configuration. Figures 2(a and b) show a series of representative optical and SEM images of the fabricated FET device with a schematic diagram of nanowires FET (Fig. 2(c)). Source-drain current versus voltage (I_{ds}–V_{ds}) measurements were carried out while varying gate voltage (V_{gs}) from −40 to 40 V. The transconductance of the devices was calculated from the slope of source-drain current versus gate voltage (I_{ds}–V_{gs}) at source-drain voltage (V_{ds}) = 1 V. Many GaN nanowire FET devices showed a degenerate behavior but a few devices exhibited full *n*-type

pinch-off. Figure 3 shows the I_{ds}–V_{ds} curve for different V_{gs} ranging from −12 to 12 V with 3 V increment for a representative GaN nanowire FET. The inset of Figure 3 shows I_{ds}–V_{gs} curve measured at V_{ds} = 1 V. The I_{ds}–V_{ds} plot shows the ohmic contact and saturation do not appear due to high carrier concentration in the nanowire.

The carrier mobility can be extracted from the following expression

$$\mu = \left(\frac{C}{L^2}V_{ds}\right)^{-1}\frac{dI_{ds}}{dV_{gs}}\bigg|_{V_{ds}=1} \quad (1)$$

where the capacitance $C = 2\pi\varepsilon\varepsilon_o L/\cosh^{-1}(1+t/r)$ by assuming a cylindrical-shaped nanowire, t is the SiO_2 layer
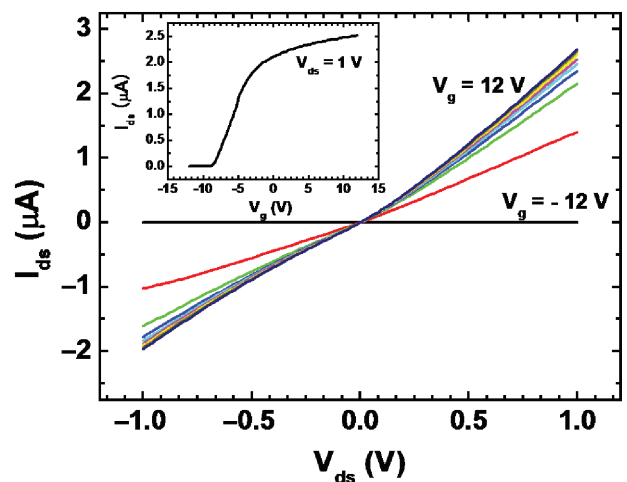
Fig. 3. I_{ds}–V_{ds} plot with various V_{gs}. The inset plot shows I_{ds}–V_{gs} at V_{ds} = 1 V.
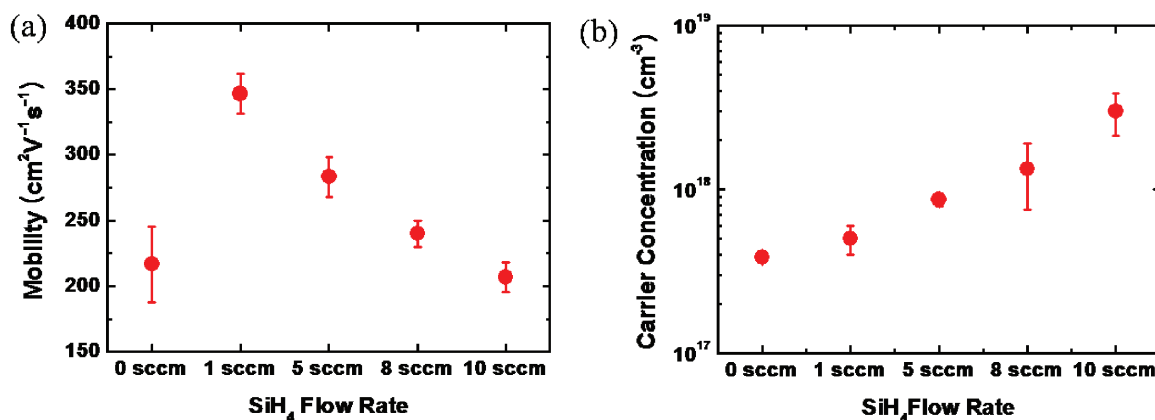
Fig. 4. Electrical properties of GaN films. (a) Plot of mobility as a function of SiH$_4$ flow rate. (b) Plot of carrier concentrations as a function of SiH$_4$ flow rate.

thickness (100 nm), r is the nanowire radius, and L is the nanowire channel length. And carrier concentration can be obtained with the mobility as $n = 1/e\rho\mu$, where e is the electronic charge and ρ is resistivity.[5] The particular nanowire FET device presented in Figure 3 yields a mobility of 105 cm^2/Vs and a carrier concentration of 4×10^{17} cm^{-3}.

In order to investigate and compare the Si doping effect in GaN films and GaN nanowires, GaN epitaxial thin films were also grown with Si doping by changing SiH$_4$ flow rate (0, 1, 5, 8, and 10 sccm). The Hall measurements were performed in the van der Pauw method to obtain carrier mobility and carrier concentration of GaN epitaxial thin films. The mobility increased when the SiH$_4$ flow rate was increased to 1 sccm, and then as the more flux of SiH$_4$ was supplied, the mobility turned to decrease, as shown in Figure 4(a). Increase of ionized Si doping causes scattering by charged Si impurities to decrease carrier mobility.[13] The initial increase of carrier mobility at small Si doping (1 sccm SiH$_4$ flux rate) is known to be the effect of increased net carrier concentration on the reduction of the Debye screening length and the edge dislocation-induced

scattering.[12] The carrier concentration increased with the increase of Si doping (SiH$_4$ flux rate), as can be seen in Figure 4(b).

Similarly, the Si doping effect on the mobility and concentration of GaN nanowires were also studied by the SiH$_4$ flow rate. Unlike the effect by Si doping on GaN films, the mobility and concentration of GaN nanowires were not quite influenced by the Si doping and SiH$_4$ flux rate, as shown in Figure 5. These GaN nanowires are highly *n*-type doped with carrier concentrations of $\sim 10^{17}$–10^{20} cm^{-3}, consistent with a previous reported result of high electron concentration in hot wall chemical vapor deposition.[5] Particularly, it was observed that device-to-device variation was very large. Large variation and negligible effect of SiH$_4$ flux rate on GaN nanowire devices can be due to the combination of surface scattering difference for different nanowires diameter, high background carrier concentration due to oxygen impurities and nitrogen vacancies, and carbon incorporation from metal-organic source.[14–17]

Micro-photoluminescence (μ-PL) of individual GaN nanowires was measured at room temperature to investigate their optical properties in the spectral range of
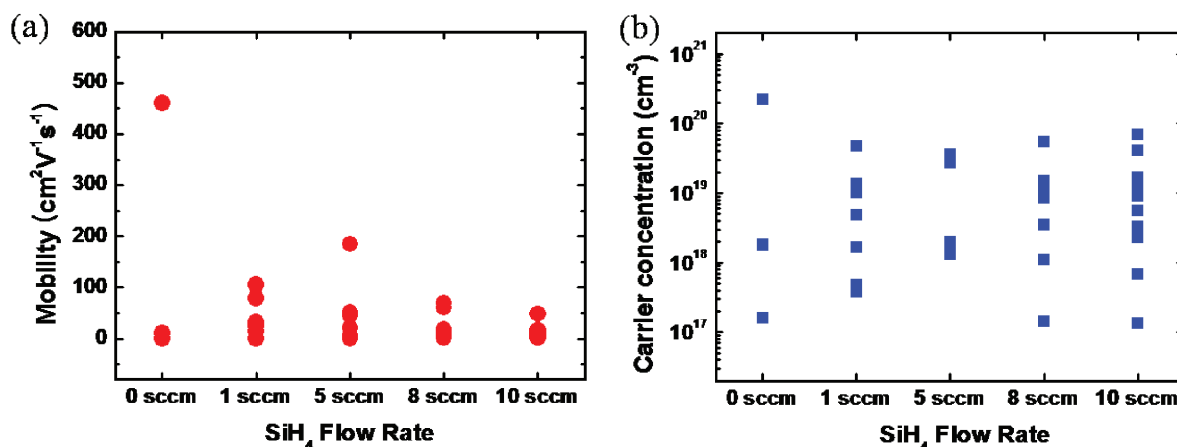
Fig. 5. Electrical properties of GaN nanowires. (a) Plot of mobility as a function of SiH$_4$ flow rate. (b) Plot of carrier concentrations as a function of SiH$_4$ flow rate.
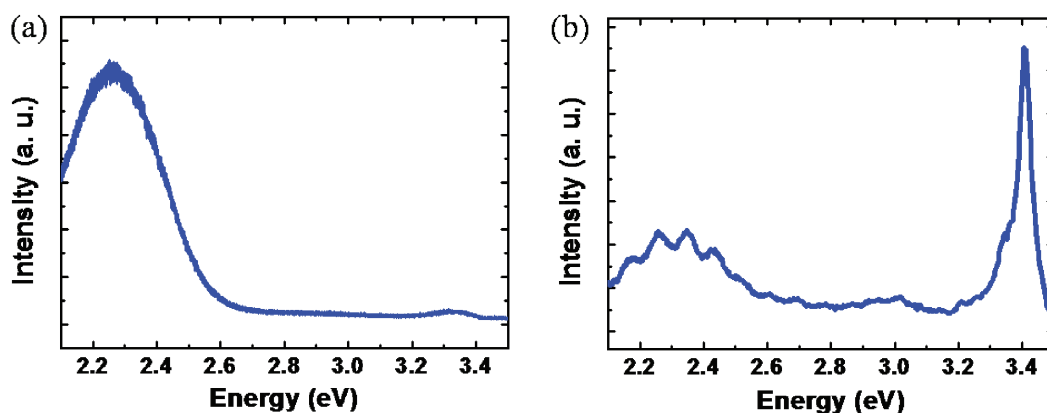
Fig. 6. (a) μ-PL spectra of single GaN nanowire. (b) PL spectra of GaN epitaxial thin films.

wavelengths from 350 to 650 nm. A typical μ-PL spectrum for individual undoped GaN nanowires is shown in Figure 6(a). Besides the band-edge emission at 3.34 eV (369 nm) and broad yellow luminescence bands in high intensity are clearly distinguishable at 2.25 eV (550 nm). The band-edge emission peak is red-shifted compared with 3.4 eV (364 nm) band-edge peak at undoped GaN films grown at same temperature (Fig. 6(b)). Dominant emission peak in GaN nanowires grown by other groups has been reported at 3.26–3.35 eV.[8, 15, 18] This red-shift from 3.40 eV in GaN film to 3.34 eV in GaN nanowires may be due to a superposition of several effects such as a Stokes shift and defect or impurity states by Ni catalyst.[8, 19] Further research is needed to deeply understand the red-shift in GaN nanowires grown by MOCVD. The oscillation in μ-PL spectrum of GaN film (around 2.2–2.5 eV range in Fig. 6(b)) is attributed to the Fabry-Perot cavity by air/GaN and GaN/sapphire in yellow luminescence. The ratio between band-edge and yellow luminescence peak intensities ($I_{\text{band-edge}}/I_{\text{yellow luminescence}}$) is 0.02–0.08 for GaN nanowires. The peak intensity ratio for GaN thin films ($\sim$2.2) is about two orders of magnitude as high as that for GaN nanowires. It has been reported that $I_{\text{band-edge}}/I_{\text{yellow luminescence}}$ ratio in Si doped GaN films decreases with increasing carrier concentration.[17] In recent studies, yellow luminescence was assigned due to complex defects involving Ga vacancies and compound of Ga vacancy and O donor, which are related to surface states.[17, 20] The yellow luminescence transition is known into compensation of *n*-type conductivity by Ga vacancies.[21] Large variation in the electrical properties of GaN nanowires can be resulted in Ga vacancies and carbon incorporation involved in yellow luminescence.

4. CONCLUSION

We have studied and compared the effect of Si doping on the electrical and optical properties of GaN nanowires and GaN films grown by metal-organic chemical vapor deposition. The Si doping was controlled by changing the

SiH$_4$ flux rate. Unlike the electrical properties of GaN films, GaN nanowire devices showed no noticeable dependence on the SiH$_4$ flux rate. The deep level intensity ratio ($I_{\text{band-edge}}/I_{\text{yellow luminescence}}$) of GaN thin films ($\sim$2.2) is about two orders of magnitude higher than that of nanowires (0.02–0.08) from photoluminescence measurements. Significant vacancies and impurities resulted in the high yellow luminescence in GaN nanowires, which leads to the large device-to-device variation, and thus to negligible dependence of Si doping and the SiH$_4$ flux rate for GaN nanowires.

References and Notes

1. Y. Huang, X. Duan, and C. M. Lieber, *Small* 1, 142 (**2005**).
2. Z. Zhong, D. Wang, Y. Cui, M. W. Bockrath, and C. M. Lieber, *Science* 302, 1377 (**2003**).
3. R. Agarwal and C. M. Lieber, *Appl. Phys. A* 85, 209 (**2006**).
4. S. Nakamura, S. Pearton, and G. Fasol, The Blue Laser Diode: The Complete Story, Springer-Verlag, Berlin (**2000**).
5. E. Cimpoiasu, E. Stern, R. Klie, R. A. Munden, G. Cheng, and M. A. Reed, *Nanotechnology* 17, 5735 (**2006**).
6. A. Cavallini, L. Polenta, M. Rossi, T. Richter, M. Marso, R. Meijers, R. Calarco, and H. Lüth, *Nano Lett.* 6, 1548 (**2006**).
7. H. Ji, M. Kuball, R. A. Burke, and J. M. Redwing, *Nanotechnology* 18, 445704 (**2007**).
8. G. Seryogin, I. Shalish, W. Moberlychan, and V. Narayanamurti, *Nanotechnology* 16, 2342 (**2005**).
9. B. S. Simpkins, P. E. Pehrsson, M. L. Taheri, and R. M. Stroud, *J. Appl. Phys.* 101, 094305 (**2007**).
10. K. A. Dick, K. Deppert, T. Mårtensson, B. Mandl, L. Samuelson, and W. Seifert, *Nano Lett.* 5, 761 (**2005**).
11. Y. Li, J. Xiang, F. Qian, S. Gradecak, Y. Wu, H. Yan, D. A. Blom, and C. M. Lieber, *Nano Lett.* 6, 1468 (**2006**).
12. M.-K. Kwon, I.-K. Park, S.-H. Baek, J.-Y. Kim, and S.-J. Park, *Phys. Stat. Sol. (a)* 202, 859 (**2005**).
13. D. G. Zhao, H. Yang, J. J. Zhu, D. S. Jiang, Z. S. Liu, S. M. Zhang, Y. T. Wang, and J. W. Liang, *Appl. Phys. Lett.* 89, 112106 (**2006**).

14. A. Motayed, M. Vaudin, A. V. Davydov, J. Melngailis, M. He, and S. N. Mohammad, *Appl. Phys. Lett.* 90, 43104 (**2007**).

15. G. T. Wang, A. A. Talin, D. J. Werder, J. R. Creighton, E. Lai, R. J. Anderson, and I. Arslan, *Nanotechnology* 17, 5773 (**2006**).

16. J. Li, L. An, C. Lu, and J. Liu, *Nano Lett.* 6, 148 (**2006**).

17. J. K. Sheu and G. C. Chi, *J. Phys.: Condens. Matter* 14, R657 (**2002**).

18. T. Kuykendall, P. Pauzauskie, S. K. Lee, Y. Zhang, and P. Yang, *Nano Lett.* 3, 1063 (**2003**).

19. J. Yoo, Y. J. Hong, S. J. An, G.-C. Yi, B. Cheon, T. Joo, J.-W. Kim, and J.-S. Lee, *Appl. Phys. Lett.* 89, 043124 (**2006**).

20. G. Li, S. J. Chua, S. J. Xu, W. Wang, P. Li, B. Beaumont, and P. Gibart, *Appl. Phys. Lett.* 74, 2821 (**1999**).

21. K. Saarinen, T. Laine, S. Kuisma, J. Nissilä, P. Hautojärvi, L. Dobrzynski, J. M. Baranowski, K. Pakula, R. Stepniewski, M. Wojdak, A. Wysmolek, T. Suski, M. Leszczynski, I. Grzegory, and S. Porowski, *Phys. Rev. Lett.* 79, 3030 (**1997**).

RESEARCH ARTICLE